

INVESTIGATION OF SEMIPOLAR GaN TEMPLATES AND InGaN MULTIPLIES QUANTUM WELLS GROWN BY HVPE AND MOVPE

SEVDA ABDULLAYEVA^{1,2}, GULNAZ GAHRAMANOVA^{1,2}, RASIM JABBAROV^{1,2},
CESARE FRIGERI³

¹*Institute of Physics, Azerbaijan National Academy of Sciences, G. Javid av., 131,
Baku 1143, Azerbaijan*

²*Research and Development Center for High Technologies, Ministry of Transport, Communication
and High Technologies of Azerbaijan Republic, 2, Inshaatchilar ave., AZ1073, Baku*

³*Institute of CNR-IMEM, Parco Area Delle Scienze, 37/A, Fontanini, Italy*

Email: gulnaz.gehremanova@hotmail.com,

In this work semipolar GaN template was grown by HVPE and semipolar InGaN QWs were grown on GaN/sapphire template by MOVPE. In order to clarify the reasons for the poor crystal quality and surface defects of semipolar GaN structures grown on sapphire wafers and we have analyzed both of samples comparatively. Via microscopic analyzes it has been obtained that the numbers of different kind of hillocks on the top of InGaN QWs are more than GaN template. TEM images showing a decreasing concentration of indium, e.g. from $x=0.200$ to $x=0.197$, from the buffer to the top of the sample. Photoluminescence peak position is not shifted with increasing excitation source power but shifted with increasing temperature from 16 K to 300 K considerably.

Keywords: III-nitrides, heterostructures, multiple quantum wells, semipolar, photoluminescence, InGaN, Atomic Force Microscopy, Transmission Electron Microscopy, Hydride Vapour Phase Epitaxy

PACS: 78.20.+e, 81.05.Ea, 81.10.+h

1. INTRODUCTION

The group of III-nitrides is widely used in many areas of our modern life: light-emitting diodes (LEDs), lasers, high electron mobility transistors (HEMTs), different type of sensors and it is some of the list of all their possible applications for the current period. The epitaxially grown InGaN wafers usually have many dislocations due to the different lattice constants and thermal expansion coefficients between the epilayer and the substrate, while InGaN nanowires can be defect-free due to different growth mechanism. Last several decades many methods have been tried to fabricate GaN structures and InGaN quantum wells (QWs) [1–5]. The GaN growth technique by MOVPE was developed in 1986 by Akasaki and H2. Amano [7]. In the early 90's modifications were made to the design of existing MOVPE tools to prevent harmful precursor and reactor flows [8, 10]. Metal-organic chemical vapor deposition (MOCVD) and molecular beam epitaxy (MBE) [11–16] were also used to grow InGaN-based nanostructures.

The first deposition of gallium nitride (GaN) was grown by hydride vapor phase epitaxy (HVPE) and investigation for optical and electrical characterization was demonstrated by Maruska and Tietjen in 1969 [17]. Kim et al. also used hydride vapor phase epitaxy (HVPE) to grow InGaN nanorods and fabricated high-brightness LED [1–4].

It is important to compare GaN template and the InGaN QWs morphology dependence of growth methods. In our previous papers [18–21] we investigated semipolar InGaN QWs which were grown by MOVPE directly. In this paper, InGaN QWs was studied with growing on semipolar GaN template which was grown by HVPE.

2. EXPERIMENT

The r-plane (10-12) sapphire substrate is used as a substrate of semipolar (11-22) InGaN MQWs. The semipolar (11-22) QWs orientation and r-plane (10-12) sapphire substrate have a tilting angle with respect to the c-plane (0001), respectively $58,4^{\circ}$ and $57,6^{\circ}$ (Fig 1a).

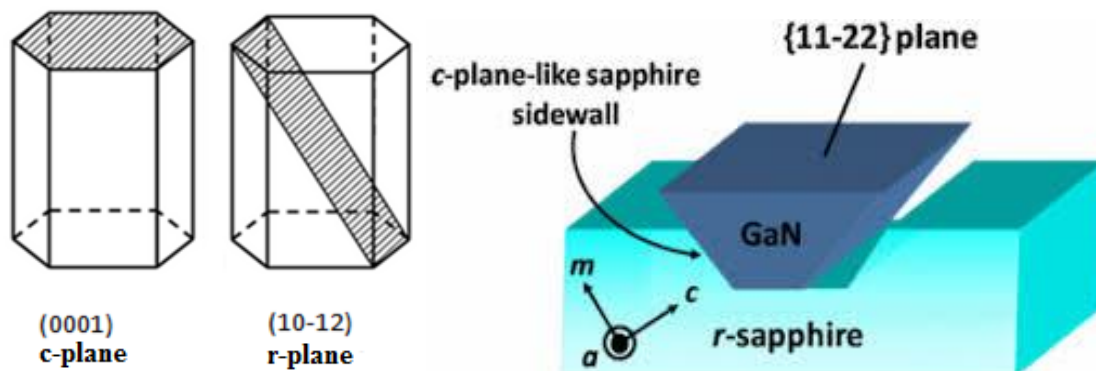


Fig. 1. a) Atomic c- and r- planes of the wurtzite crystal. b) Illustrate of semipolar (11-22) GaN growth direction at the inclined c-plane-like sidewalls (schematically).

The photolithography process was done for tilting the substrate. For this purpose a negative photoresist (PR) has been used on the rotated substrate and the thin photoresist was spread on the substrate. After covering about $1.7\mu\text{m}$ thick PR the substrate by photoresist it was baked during two minutes. In the next step the PR was exposed by the UV light. Therefore, the exposed parts of the photoresist become less soluble in chemical developer. The unexposed parts of the photoresist are removed by chemical developer. In the next step via Reactive Ion Etching (RIE) the samples were etched in chosen optimal pressure and etching time. Hence, the stripes get transferred into the sapphire substrate and the

desired angle ($58,4^{\circ}$) of trench side -wall was achieved (Fig. 1b). After RIE, in order to remove the photoresist mask stripes on the substrate first oxygen plasma cleaning was done. Then in the chemical solutions of KOH and H_2O and H_2SO_4 and H_2O_2 the substrate was cleaned completely from residuals. Then the silicon dioxide (SiO_2) was sputtered on top of the sample (or c-plane facet) a mask to get covered with SiO_2 to avoid parasitic growth. Thus, in order to structure the (10-12) oriented sapphire, at first about $1.7\mu\text{m}$ thick layer of a negative photoresist is spin-coated on it. The photoresist itself is patterned by optical lithography with a stripe shadow mask with an opening of $3\mu\text{m}$ and a period of $6\mu\text{m}$.

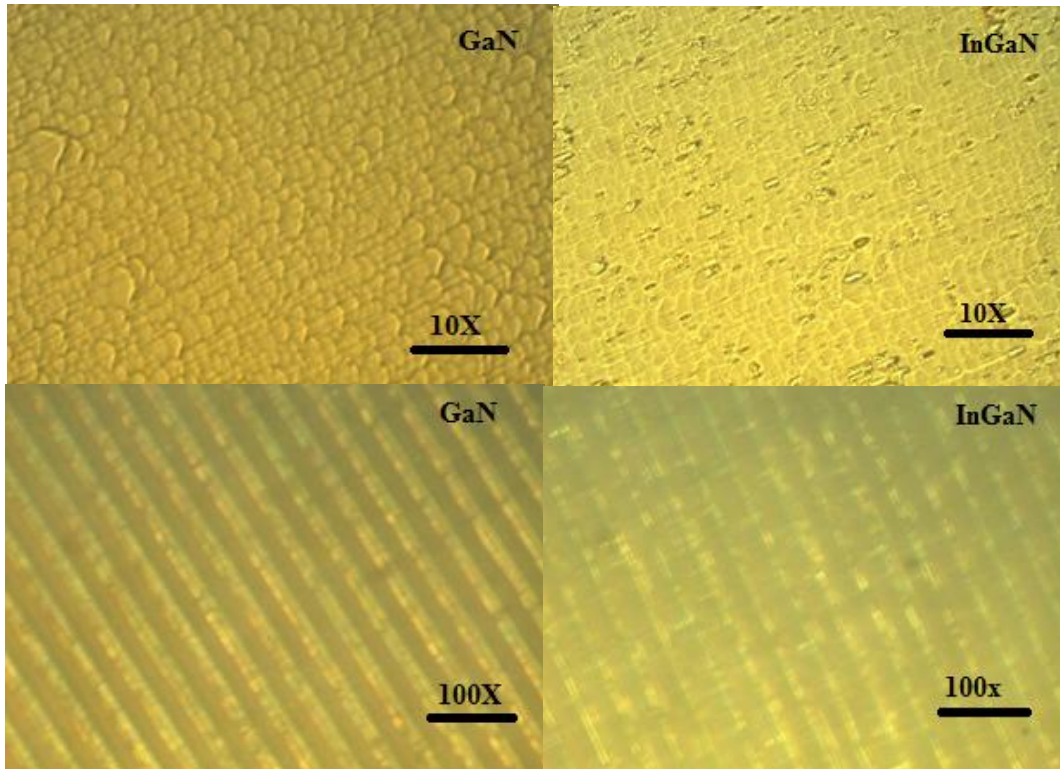


Fig. 2. Optic Microscopy images a)GaN -10x, b)InGaN- 10x, c)GaN-100x, d)InGaN-100x.

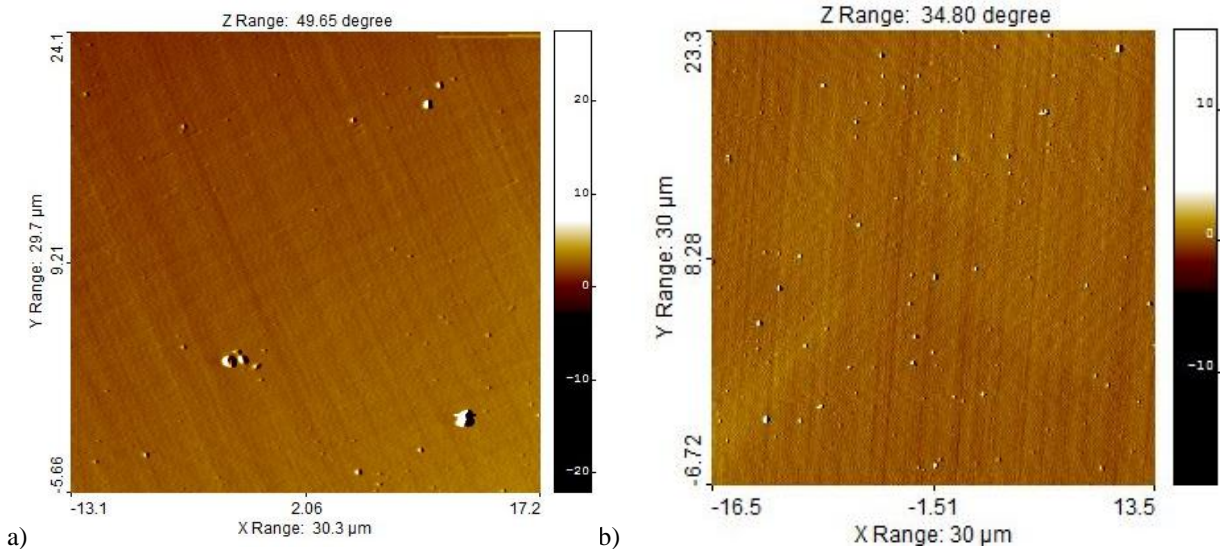


Fig. 3. Atomic force microscopy scans of structures. Morphology and surface defects of semipolar GaN template (left) and InGaN/GaN MQWs heterostructures (right) on $30 \times 30\mu\text{m}^2$ surface area.

The growth of GaN buffer layer on the patterned sapphire substrate was performed by HVPE. The growth was done in a commercial Aixtron single-wafer HVPE system with a horizontal quartz-tube [15, 16]. Approximately 4µm thick GaN layer has been deposited at a fairly low growth temperature of 900– 970 °C. We called this template “GaN template”.

In the following stage the 5 period InGaN/GaN MQWs heterojunctions have been deposited on the top of HVPE growth GaN by MOVPE. The MOVPE growth was done in a commercial Aixtron-200/4 RF-S HT reactor using the standard precursors: ammonia (NH₃), trimethylgallium (TMGa), trimethylindium (TMIn) and triethylgallium (TEGa). In order to achieve fairly long wavelength above 500 nm, the InGaN MQWs were grown at a temperature of typically 720°C (58 s) , while the temperature was increased by about 35°C for the GaN barrier growth (104 s). At the end of growth process the thin GaN top layer was deposited during 10 second on top of 5 period InGaN/GaN heterojunctions.

3. RESULTS AND DISCUSSIONS

In figure 2, the Optical Microscopy images were described for GaN template and InGaN MWQs. As shown in Fig. 2 c and d the c-directions patterns is visible on GaN before growing InGaN QWs, bur after growing InGaN MQWs because of QWs cover on the top of GaN template the pattern lines were disturbed. It is usually accepted that the high defect density in GaN leads to poor optical property and also affects the structural and optical quality of the active layer composed of the InGaN/GaN MQWs. Well-defined, uniform and long crystallographic steps could be observed on the surface by AFM. The undesirable growths with surface hillock can be seen from AFM 2D images (Fig. 3). The intersection of a screw-component dislocation with the film surface creates an atomic step termination that may lead to hillock formation (Burton et al 1951).

The presence of clustered defects with the screw component of the Burgers vector is a reason of formation of the growth hillocks. More growth hillocks located at the top and some pits located away from the hillock peaks, are shown in Fig. 3(a, b). On the top of InGaN QWs the numbers of different kind of hillocks are more than GaN template. It means them come from MOVPE growth conditions. Remarkable morphological differences are noticeable for GaN template and InGaN QWs on the same GaN template.

The semipolar InGaN MQWs have been investigated by TEM. TEM observations were carried out on a cross sectional specimen, i.e. along a direction orthogonal to the growth direction. This is the only way to detect the QW layers individually and measure their individual composition. To this aim two different TEM

operation modes were used, namely HR-TEM (high resolution TEM) and HAADF (high angle annular dark field) modes. The HR-TEM mode is the usual way to get images with atomic resolution, by exploiting the interference of all the electron beams diffracted by the lattice planes of the specimen, according to the Bragg law. In HR-TEM mode the parallel illumination of the specimen is used.

The HAADF mode is instead based on the Rutherford-like scattering, by the atoms of the specimen, of the electrons of the incident beam when it crosses the specimen. Here the TEM electron beam is focused to a small size (0.5-0-7 nm in our case) and is scanned across the sample, like in an SEM: the TEM is operated in the Scanning mode, i.e. STEM mode. Most importantly in our case, the mentioned scattering goes as Z^n , with Z the average atomic number of the investigated region and $1.7 < n < 2$. The higher Z the higher is the scattering angle [18]. The most accepted value is $n=2$. By using a post-specimen annular detector around the TEM optical axis one can collect the scattered beams whose intensity increases with increasing Z. Materials with high average Z give brighter contrast than those with low average Z. HAADF thus gives a chemical information about the specimen (sample) composition.

The InGaN QWs region (including the cap) is between the 2 yellow arrows (Fig 4a, b). The blue encircled bright lines in the GaN beneath the QW layers are very likely twins. Such defects generally originate at the interface (IF) with the substrate. However, it is not possible to confirm this here as the GaN/Al₂O₃ IF is not visible. On this sample the HAADF intensity is proportional to Z^n (Z atomic number of the analysed sample).

Hence it is

$$\begin{aligned} \text{- for In}_x\text{Ga}_{1-x}\text{N} \quad I_{IGN} &= x Z_{In}^n + (1-x) Z_{Ga}^n + Z_N^n \\ \text{- for GaN} \quad I_{GN} &= Z_{Ga}^n + Z_N^n \end{aligned}$$

The concentration x of In in an In_xGa_{1-x}N layer can be obtained from the ratio A of the two net experimental intensities,

$$A = I_{IGN} / I_{GN}$$

and is given by, for $n=1.7$, $x = 0.915 (A-1)$. Results on x are reported in the table. The error was 7-10%.

This may support the calculations performed on the HAADF images showing a decreasing concentration of In, e.g. from $x=0.197$ to $x=0.200$, from the buffer to the top of the sample. : Intensity profile from bottom to top of the QWs structure along the arrow in numbers help to establish the link between image and profile (Fig 5).

In _x Ga _{1-x} N (Number of QWs)	1	2	3	4	5
X (concentration of In)	0.200	0.209	0.199	0.174	0.197

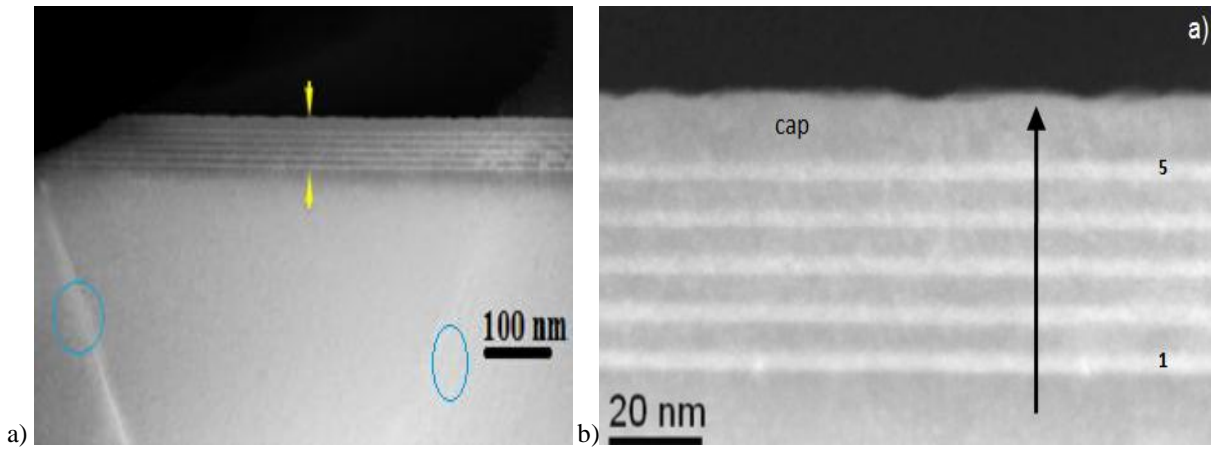


Fig. 4. TEM images: High angle annular dark field (HAADF) scanning transmission electron microscopy (STEM) of semipolar InGaN QWs on the top of GaN template.



Fig. 5. HAADF image: Intensity profile from bottom to top of the QWs structure along the arrow in numbers help to establish the link between image and profile.

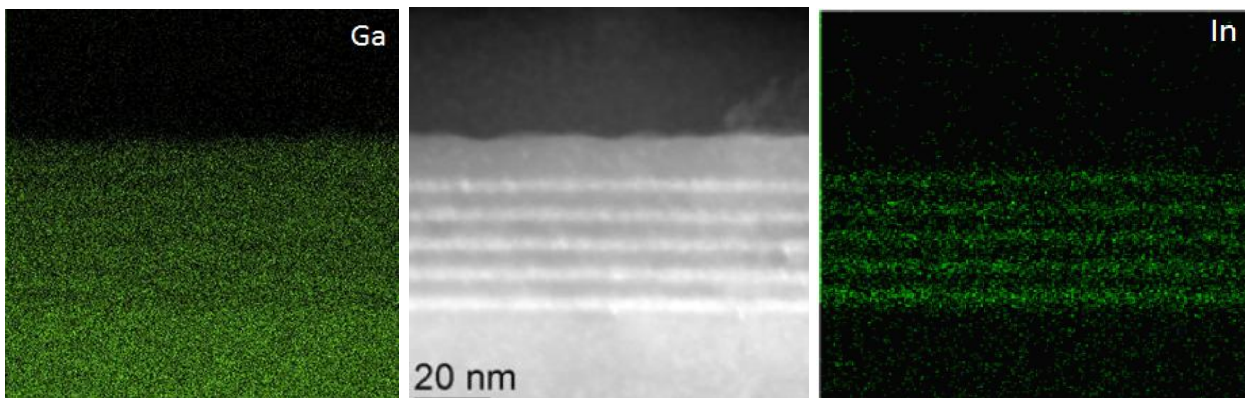


Fig. 6. Energy-dispersive X-ray spectroscopy (X-EDS) maps of InGaN QWs.

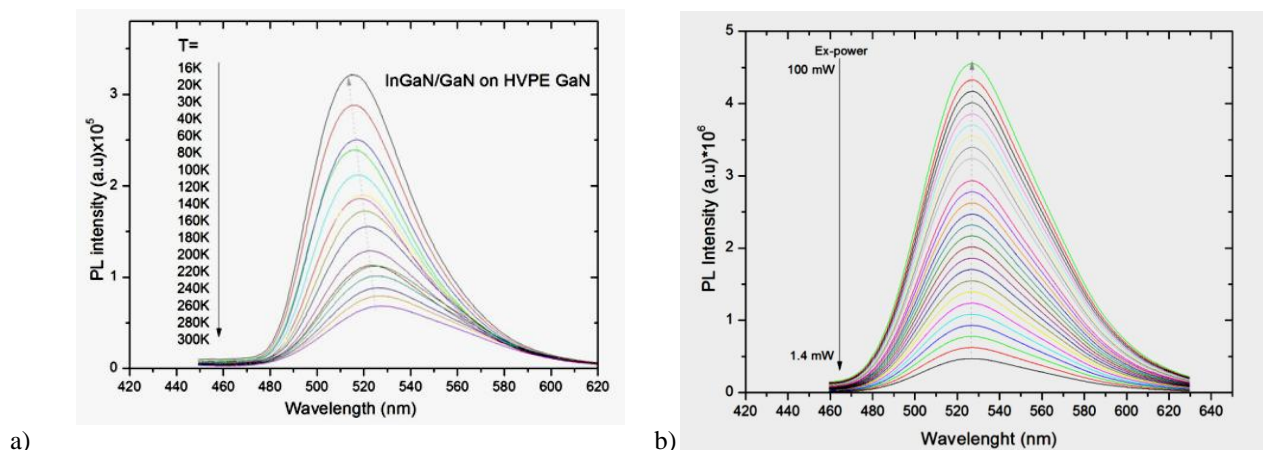


Fig. 7. PL characterization of InGaN QWs sample at different temperatures (a) and excitation power sources (b).

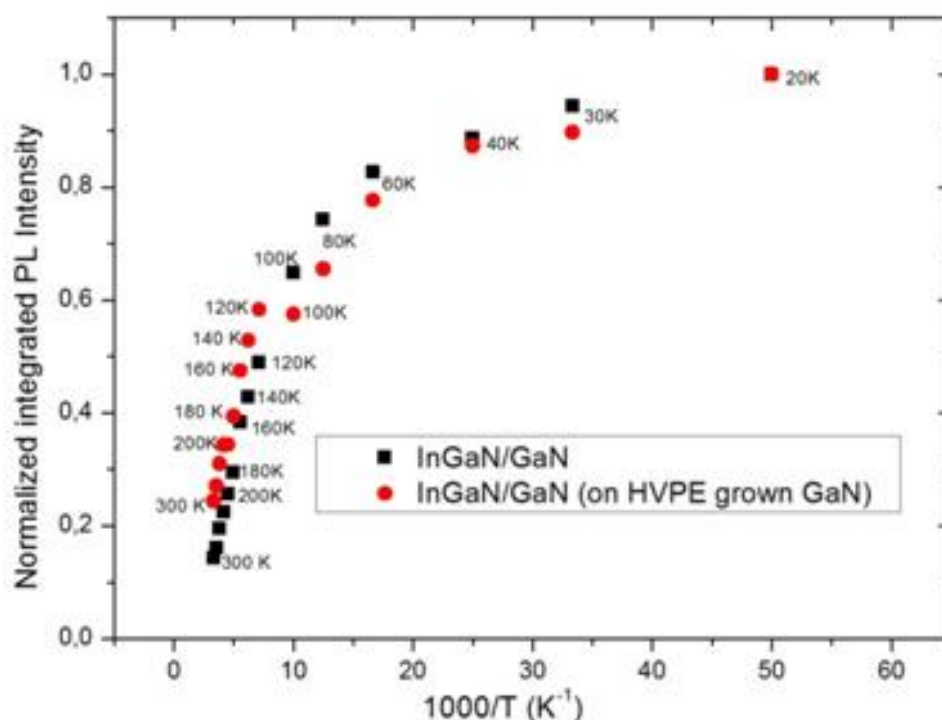


Fig. 8. Arrhenius plot of the normalized integrated PL intensity of InGaN MQWs samples.

X-EDS (Energy-dispersive X-ray spectroscopy) is a method able to give chemical information about the composition of a specimen investigated by TEM. Here the middle image is the HAADF image of the InGaN QWs like the one in fig. 6 a). On the left is the X-EDS map of Ga while on the right is the one of In. Pretty evident is the correspondence between the In rich layers and the 5 brighter layers in the HAADF image, confirming the identification of the brightest layers as InGaN as deduced from the HAADF measurements. A weak depletion of Ga in correspondence of the In rich layers is also detectable. In the X-EDS map for In (right) the 1st InGaN layer from the buffer is brighter than all the others. The other 4 ones are also less and less bright on moving to the top (Fig. 6).

PL emission intensity was significantly decreased linearly with increasing measurement temperature and excitation power respectively Fig. 7a and Fig. 7b. PL peak³

position is not shifted with increasing excitation source power but shifted with increasing temperature from 16 K to 300 K considerably.

At the end we compared the temperature dependence of the normalized integrated PL intensity of this sample with other InGaN QWs sample with was grown by MOVPE directly. (Fig. 8). The integrated PL intensity falls gradually in two samples with increasing temperature. These results could be explained due to increasing non-radiative recombination path in these structures. Assuming that the internal quantum efficiency (η_{int}) identical and equals unity at 16 K, we obtain η_{int} of 0.15 and 0.24 at room temperature for our current investigated InGaN QWs sample (on HVPE grown GaN/Al₂O₃ template) and other InGaN QWs (grown directly on sapphire by MOVPE) respectively.

4. CONCLUSION

We have investigated surface defects of semipolar GaN template grown on patterned sapphire wafers by HVPE and semipolar InGaN QWs on the top of this GaN/sapphire template. AFM, TEM, X-EDS and PL characterizations were done of QWs. Via microscopic analyzes it has been obtained that on the top of InGaN QWs the numbers of different kind of hillocks are more than GaN template. HAADF images showing a decreasing concentration of In, e.g. from $x=0.197$ to $x=0.200$, from the buffer to the top of the sample. PL peak position is not shifted with increasing excitation source power but shifted with increasing temperature from 16 K to 300 K considerably. The internal quantum efficiency for our current investigated InGaN QWs

sample (on HVPE grown GaN/sapphire template) and other InGaN QWs (grown directly on sapphire by MOVPE) are identical and equals unity at 16 K. At the room temperature the internal quantum efficiency of our current investigated InGaN QWs (on HVPE grown GaN/sapphire template) was higher than second sample, 0.24 and 0.15 respectively.

ACKNOWLEDGMENT

We are grateful to Prof. Dr. Ferdinand Scholz (Ulm University, Germany) for the possibility to carry out the main part of this work in his GaN group at the Institute of Optoelectronic and for him strong technical and scientific support. This work has been partly financially supported by the German Academic Exchange Service (DAAD).

-
- [1] H.M. Kim, T.W. Kang, K.S. Chung. J. Ceram. Proc. Res. 5 (2004) 241–243.
- [2] H.M. Kim, Y.H. Cho, H. Lee, S. Kim II, S.R. Ryu, D.Y. Kim, T.W. Kang, K.S. Chung. Nano Lett. 4 (2004) 1059–1062.
- [3] H.M. Kim, H. Lee, S. Kim II, S.R. Ryu, T.W. Kang, K.S. Chung. Phys.Stat. Sol. (b) 241 (2004) 2802–2805.
- [4] Y. Sun, Y.H. Cho, H.M. Kim, T.W. Kang. Appl. Phys. Lett. 87 (2005),093115-1-093115-3.
- [5] F. Qian, S. Gradečak, Y. Li, C.Y. Wen, C.M. Lieber. Nano Lett. 5 (2005)2287–2291.
- [6] F. Qian, Y. Li, S. Gradečak, D. Wang, C.J. Barrelet, C.M. Lieber. Nano Lett. 4 (2004) 1975–1979.
- [7] T.H. Hsueh, H.W. Huang, C.C. Kao, Y.H. Chang, M.C. Ou-Yang, H.C.Kuo, S.C. Wang. J. J. Appl. Phys. 44 (2005) 2661–2663.
- [8] H. Amano, N. Sawaki, I. Akasaki and Y. Toyoda. Appl. Phys. Lett. 48, 353(1986).
- [9] S. Nakamura and G. Fasol. The Blue Laser Diode (Springer Verlag, 1997).
- [10] S. Nakamura. Jpn. J. Appl. Phys. 30, 1348 (1991).
- [11] Y. Wang, K. Zang, S. Chua, M.S. Sander, S. Tripathy, C.G. Fonstad. J.Phys. Chem. B 110 (2006) 11081–11087.
- [12] A. Chen, S.J. Chua, P. Chen, X.Y. Chen, L.K. Jian. Nanotechnology 17 (2006) 3903–3908.
- [13] P. Chen, S.J. Chua, Y.D. Wang, M.D. Sander, C.G. Fonstad. Appl. Phys.Lett. 87 (2005), 143111-1-143111-3.
- [14] A. Kikuchi, M. Kawai, M. Tada, K. Kishino. J. J. Appl. Phys. 43 (2004) L1524–L1526.
- [15] G. Pozina, J.P. Bergman, B. Monemar, V.V. Mamutin, T.V. Shubina, V.A. Vekshin, A.A. Toropov, S.V. Ivanov, M. Karlsteen, M. Willander. Phys.Stat. Sol. (b) 216 (1999) 445–450.
- [16] T. Kouno, A. Kikuchi, K. Kishino. Phys. Stat. Sol. (b) 243 (2006)1481–1485.
- [17] Y.H. Kim, J.Y. Lee, S.H. Lee, J.E. Oh, H.S. Lee, Y. Huh. Chem. Phys. Lett.412 (2005) 454–458.
- [18] Caliebe, T. Meisch, B. Neuschl, S. Bauer, J. Helbing, D. Beck, K. Thonke, M. Klein, D. Heinz and F. Scholz. Phys. Status Solidi C 11, 525–529 (2014).
- [19] T. Walther, J. Microsc. 221, 137 (2006) and C. Frigeri et al., Nano. Res. Lett. 6, 194 (2011).
- [20] H.P. Maruska. Appl. Phys. Lett., vol. 15, no. 10, p. 327,1969.
- [21] F. Scholz, M. Caliebe, G. Gahramanova et. al. Phys. Status Solidi B, 2016, v.253,No1, pp. 13–22
- [22] S. Abdullayeva, G. Gahramanova, R. Jabbarov. Azerbaijan Journal ofPhysics, 2015, v. XXI, No 4, Section: En, pp. 47-51.
- [23] S. Abdullayeva, G. Gahramanova, R. Jabbarov, T. Orujov. Azerbaijan Journal of Physics, Volume XXII, No 1, Section: En,2016, p. 49–51.
- [24] S. Abdullayeva, G. Gahramanova, Cesare Frigeri, N. Musayeva, R. Jabbarov. International Scientific Conference on Sustainable Development Goals-2017, 24-25 November, Baku, 2017, pp. 391-395

Received: